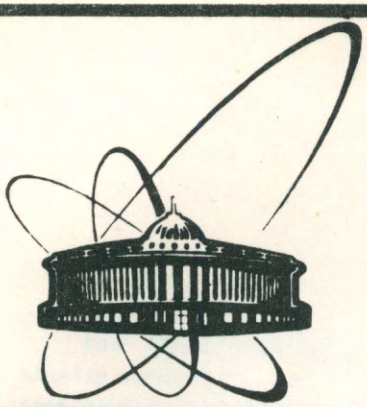

объединенный
институт
ядерных
исследований
дубна

E1-89-257

G.D.Alekseev, M.S.Bilenky, Yu.Ye.Bonyushkin,
A.V.Korytov

STUDIES OF THE STABILITY AND SYSTEMATICS OF OPERATION OF THE DELPHI PLASTIC STREAMER TUBES

Submitted to "Nuclear Instruments and Methods in Physics Research"

1989

1. Introduction.

The DELPHI hadron calorimeter[1] includes about 20,000 plastic steamer tubes[2] as active detectors in gaps between 5cm iron layers. The schematic view of a DELPHI plastic streamer tube is shown in fig.1. The detector length is from 30 cm to 4 m and the cathode resistivity is in the range 50-2000 kOhm per square. A specific feature of the DELPHI tubes is that the graphite cathode surface is mechanically polished. This procedure increases their operational stability[3]. Signals are picked up by external pads ~20×20 cm^2 in size.

Here we present the results of the study of the operation stability and the response deviations of the DELPHI streamer tubes under different conditions. Many of this questions have already been considered elsewhere[4,5,6]. The presented results are considered from the point of view of using the detectors in the DELPHI hadron calorimeter. The intrinsic energy resolution of the DELPHI calorimeter at 100 GeV is expected to be

$$\frac{80\%-100\%}{\sqrt{100}} = 8-10\%.$$

So the additional contributions due to changes of the tube response should be kept below this level.

The measurement conditions were identical through the whole work. The pulse shaping time was 450 ns and the threshold was 15 mV / 50 Ohm for the singles rate. The integration time was 300 ns for the collected charge characteristics. The tubes were irradiated by the ^{90}Sr β-source, except for specified cases.

Fig.1. Schematic drawing of the plastic streamer tube for the DELPHI hadron calorimeter: 1 - container, 2 - cover, 3 - 80 μm Be-Cu anode wire, 4 - profile with eight 9x9 mm^2 cells and 1 mm walls.

2. Choice of Gas Mixture.

To decrease problems of external induced currents and to simplify the readout electronics it is preferable to use a large gas gain in detectors, i.e. the self-quenching streamer (SQS) mode. But operation in the SQS mode requires rather large organic percentage in the gas mixture. The "standard" mixture for the operation of the tubes in this mode is Ar:i-C_4H_{10}=1:3. However, in the underground experiments with large detector volume (the DELPHI hadron calorimeter contains about 40 m^3 of gas), one has to reduce the hydrocarbon content for safety reasons. An usual compromise decision is to replace a large part of hydrocarbon with CO_2 /7,8,9/. Mixtures without flammable gases (for example, with pure CO_2 /10,11/) were also tested. This was found not to ensure the stable operation with large gas gains (the maximum mean streamer charge is not larger than 5-30 pC).

Besides, gas mixtures giving a small slope of a charge characteristic (lgQ vs high voltage) are preferable. A smaller slope means better quenching property of the gas mixture. This provides a longer plateau of the singles rate curve. Detectors with such mixtures are less sensitive to many types of geometric deviations (see section 9). The charge characteristics obtained

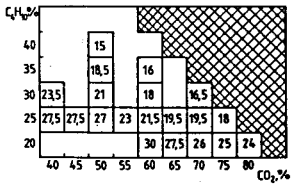

Fig.2. The investigated concentrations of the Ar:Co_2:i-C_4H_{10} gas mixture. The figures in squares represent the slopes of the charge characteristics for the streamer mode in dB/kV.

Fig.3. The singles rates (cosmics) for different concentrations of the Ar:CO_2:i-C_4H_{10} gas mixture:

a)1.20:60:20
2.15:65:20
3.10:70:20
4. 5:75:20
5. 0:80:20

b)1. 35:40:25
2. 30:45:25
3. 25:50:25
4. 20:55:25
5. 15:60:25
6. 10:65:25
7. 5:70:25
8. 0:75:25

c)1.30:40:30
2.20:50:30
3.10:60:30
4. 0:70:30

with these mixtures are smoother, have no large leaps in the transition region from the limited proportional mode to the SQS one. So if necessary, it gives an opportunity to decrease the gas gain without a large break in the charge characteristic (see section 8).

To choose the optimal gas mixture, different variants of the mixture Ar:CO_2:i-C_4H_{10} /22/ and the mixture Ar:CO_2:n-C_5H_{12}=25:50:25 were systematically studied.

Fig. 2 shows all tested proportions of the Ar:CO_2:i-C_4H_{10} mixture. Each tested mixture is represented by a square on the plane of the independent variables (%CO_2; %C_4H_{10}). The figures in squares are slopes of change characteristic (dB/kV). The singles rates and the charge characteristics for the majority of these mixtures are represented in fig.3,4.

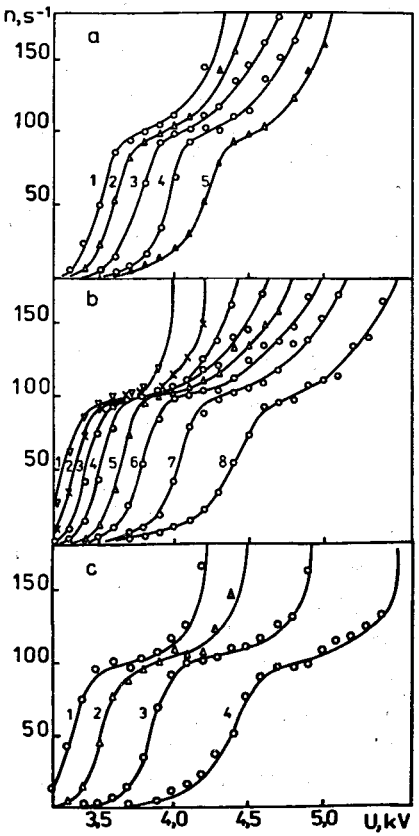

These data allow the following conolusions :

1) the larger the percentage of $i\text{-}C_4H_{10}$ and CO_2 (in smaller degree) the longer the plateau of the singles rate curve;

2) the larger the percentage of $i\text{-}C_4H_{10}$ and CO_2 (in smaller degree) the smaller the slope of the charge characteristic (fig 5);

3) too large part of CO_2 gives rise to afterpulses.

Gas mixtures were also compared in a large group of detectors (60 streamer tubes 3,5m long). Fig.6 represents the curves showing the fraction of operating detectors vs the high voltage for different amount of CO_2 in the gas mixture (amount of C_4H_{10} is 25%) under cosmic radiation. The abscissae represents the range of operating high voltage. We define this voltage as the one counted from 80% efficiency point, where singles rate curve still has a sufficiently sharp rise (this permits determination of the initial point with a good accuracy).

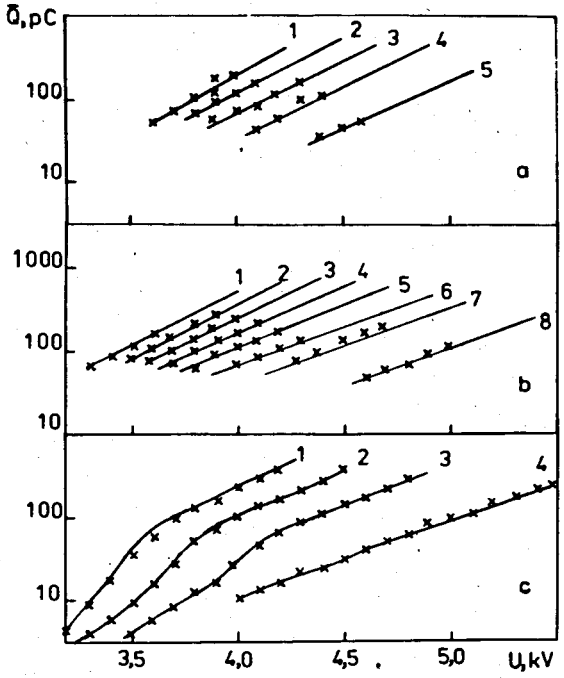

Fig.4. The charge characteristics (cosmics) for different concentrations of the $Ar:CO_2:i\text{-}C_4H_{10}$ gas mixture (the numbers indicate the same concentrations as in fig.3)

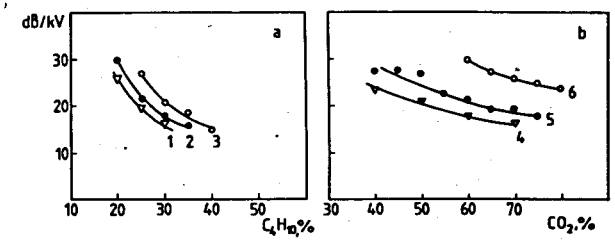

Fig.5. The charge characteristic slope vs the concentration of $i\text{-}C_4H_{10}$ (a) and CO_2 (b) in the $Ar:CO_2:C_4H_{10}$ gas mixture: a) 1 - 70% CO_2, 2 - 60% CO_2, 3 - 50% CO_2, b) 4 - 30% $i\text{-}C_4H_{10}$, 5 - 25% $i\text{-}C_4H_{10}$, 6 - 20% $i\text{-}C_4H_{10}$.

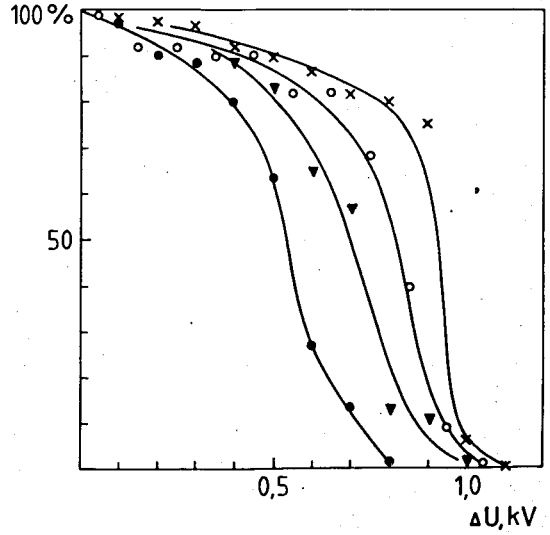

Fig.6. The fraction of the operating tubes vs the high voltage under cosmic radiation (a tube was considered as an operating one if its dark current was less than 1 μA). 100% correspond to 60 tubes 3.5 m long. $\Delta U=U-U_i$, where U_i corresponds to the 80% efficiency. The $Ar:CO_2:C_4H_{10}$ gas mixtures (35:40:25(•), 25:50:25 (▾), 15:60:25(•), 5:70:25(×)) were used.

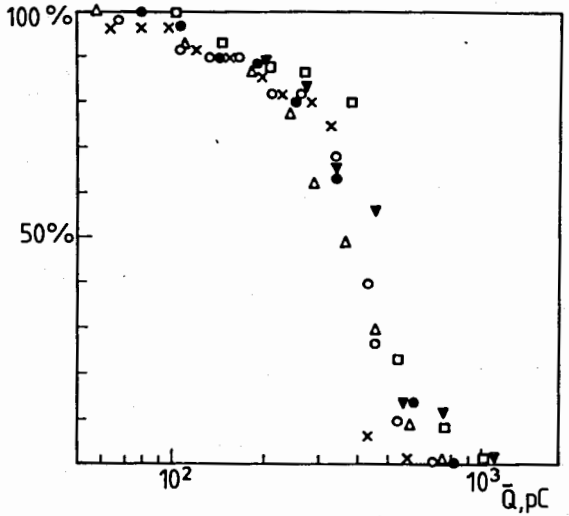

Fig.7. The fraction of the operating tubes vs the mean streamer charge. The Ar:CO_2:i-C_4H_{10} gas mixtures (35:40:25(•), 25:50:25(▾), 15:60:25(●), 5:70:25(×), 20:60:20(▫)) and the gas mixture Ar:CO_2:n-C_5H_{12}=25:50:25(△)were used. Signals were generated by the cosmic radiation.

Detectors were rejected if dark current (current mainly due to self-sustaining discharges) exceeded 1 μA. In fig.6 one can clearly see that at this definition of the operating high voltage range (from the 80% efficiency to the 1 μA dark current) a gas mixture with more CO_2 (with the fixed i-C_4H_{10} part) is more preferable.

The data represented in fig.7 should be specially emphasized. Fig.7 shows the fraction of the operating detectors vs the mean steamer change value for different gas mixtures (including that with n-Pentane - Ar:CO_2:n-C_5H_{12}=25:50:25). Statistics is the same: 100% refer to 60 detectors. For the mixtures used the specific charge scaling was observed, i.e. the maximum possible charge of these detectors does not depend on percentage composition of the gas mixture Ar:CO_2:C_4H_{10} and on replacement of i-C_4H_{10} by n-C_5H_{12}. The scaling for different concentrations of n-Pentane in the gas mixture Ar:CO_2:n-C_5H_{12} was also observed in the paper[9] for one detector (the end of the operating range was defined as the point

at which afterpulses follow the main streamer signal by more than 15% of the total counts).

From fig.7 one may conclude that the DELPHI plastic streamer tubes should operate rather reliably up to streamer charge ~100 pC. If the charge is near to ~1000 pC, these detectors do not practically operate.

It should be noted that the similar values of the maximum charges ~100-1000 pC for the streamer mode were observed in the wire cathode chambers[12]. It may be connected with appearance of self-sustaining dischargers due to electrons taken away from the cathode by ions. The charge of 100 pC corresponds to the number of ions M~10^9 and a typical probability of taking away an electron from the cathode by an ion γ is about 10^{-9} [13]. Thus the Townsend condition for appearance of a self-sustaining discharge M·γ≃1 is satisfied for charges ≃100 pC.

Here it is important to note that n-Pentane is a more flammable gas then Isobutane and since it does not provide larger charges it is less suited for the big underground setup. Keeping in mind that the safety reasons confine us to mixtures with no more than 30% of a flammable gas one may conclude that the mixture Ar:CO_2:C_4H_{10}=10:60:30 providing a small slope of the charge characteristic, not very high operation voltage and yielding almost no afterpulses is close to the optimum.

3. Self-sustaining Discharge

It is well known that in plastic streamer tubes with rather large surface resistivity local rates exceeding ~10 particles/cm^2·s may provoke self-sustaining discharges.[14,15] To increase the operation stability the DELPHI tubes were first polished, as mentioned in the Introduction, and then they were tested[16] during the mass production with the cosmics and the X-ray source (the scanning was carried out so that each surface point was irradiated with the intensity ~1000 $cm^{-2}c^{-1}$ for 0.1 s).

However the possibility of a self-sustaining discharge cannot be excluded in the real experimental conditions. Hence it is important to know whether a tube with a self-sustaining discharge poisons the gas so that the next tubes change essentially their characteristics.

It was checked in the following way. Three short (~30 cm) tubes were flowed with the gas mixture Ar:CO_2:C_4H_{10}=10:60:30. They

were connected in series. The flow rate was similar to the gas rate for the DELPHI hadron calorimeter (~20 cm^3/min through a tube). A self-sustaining discharge with the ~10 μA current was provoked in the second tube.

For two days the charge characteristics of the first and the third tubes were compared. No noticeable change in operation were found (charge differences were within the measurement accuracy level of 2%).

Thus the self-sustaining currents of ~10 μA do not considerably change the gas medium and do not apparently lead to self-sustaining currents in the next tubes.

4. Detector Aging.

The irradiation-caused aging effect[17] is a common feature of wire gaseous chambers. This problem demands a special attention in the case of large detectors supposed to operate for many years.

The DELPHI plastic streamer tubes were investigated under the following conditions. We used the gas mixture $Ar:CO_2:i\text{-}C_4H_{10}$= =10:60:30 with the flow rate of 120 cm^3/min. Two-centimeter sections of all 8 wires were irradiated with ^{90}Sr, i.e. 8×2=16 cm of wire were irradiated. The initial streamer charge was about 100 pC and β-source intensity of ~5×10^3 particles/$cm^2\cdot s$. To avoid the influence of the changes in the atmospheric pressure, temperature and slight changes in the gas mixture, aging detector data were compared with the reference detector data. The reference detector was placed before the aging one under the same gas flow.

The streamer charge drop is shown in fig.8. A slop is about 0.12%/(mC/cm).

A modification of singles rate curves is shown in fig.9. It is seen that the plateau beginning moves to higher voltages as the charges accumulates. It is apparently connected with the polymerization processes on the anode wire. The plateau end moves to lower voltages and it is apparently connected with the Malter

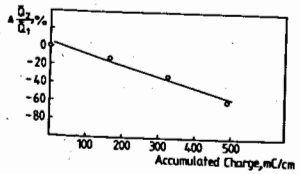

Fig.8. The streamer charge drop with the aging of the DELPHI plastic streamer tube.

effect due to attachment of polymers to the cathode. Point 4.1 kV (the knee of the singles rate curve) became non-operational after the total charge about 560 mC/cm was accumulated.

Assuming that radiation conditions for streamer tubes in the DELPHI hadron calorimeter will be as hard as 1 particle/$cm^2\cdot s$, one may extrapolate the obtained aging data to the lifetime of the calorimeter. Thus, one may expect the signal drop to be about 0.06% per year and the estimated detector lifetime to be about 1000 years if the detectors operate at 4.1 kV.

Here it should be noted that the aging processes are sensitive to the conditions of the aging[17] (gas flow, gas gain, irradiation intensity etc.) and the test conditions always differ from the real experiment.

However, even taking into account this fact our estimations allow us to hope that the aging effects for the DELPHI tubes will be negligible.

5. Signal Changes Due to the Magnetic Field.

The magnetic field may affect not only the hadron shower development[18] but also the streamer charge[19]. These effects may lead to the systematic difference between the calorimeter responses for hadrons flying out at different angles. The estimated difference between the barrel and end-cap responses is about 20-30% (the major part is due to the influence of the field on the shower development, its influence on the streamer charge itself is about several percent).

This systematics can be eliminated by the direct calibration of the calorimeter with a magnetic field.

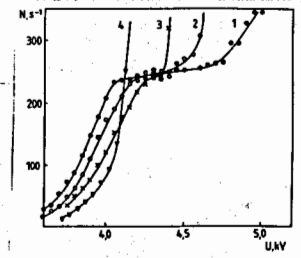

Fig.9. The singles rate curve transformations with the aging. The figures correspond to the total accumulated charges: 0 mC/cm (1), 330 mC/cm (2), 490 mC/cm (3), 560 mC/cm (4).

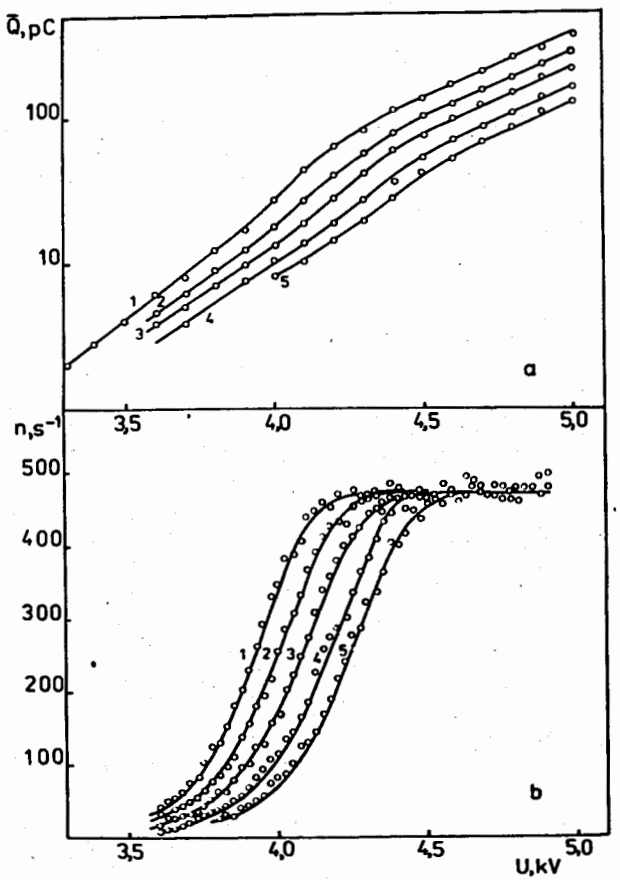

Fig.10. The charge characteristic transformations (a) and the singles rate shifts (b) vs the pressure increase: 766 Torr (1), 798 Torr (2), 827 Torr (3), 864 Torr (4), 893 Torr (5).

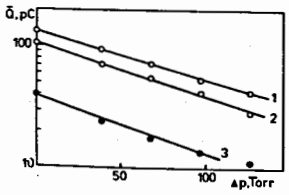

Fig.11. The mean streamer charge change vs the pressure increase. It may be fitted by an exponential function: $\bar{Q} = \text{const} \cdot \exp(-\beta \cdot \Delta p)$. 1 - U = 4.5 kV; $\beta = 9.0 \cdot 10^{-3}$/Torr; 2 - U = 4.4 kV, $\beta = 9.9 \cdot 10^{-3}$/Torr; 3 - U = 4.1 kV, $\beta = 10.6 \cdot 10^{-3}$/Torr.

6. Pressure, Temperature and High Voltage Instability Influence.

The measurements had shown the strong dependence of the streamer charge on pressure[8]. The changes in the charge characteristics and the shift of the singles rate curves measured by us with increasing pressure are presented in fig.10 (the gas mixture was $Ar:CO_2:i\text{-}C_4H_{10}=10:60:30$). Fig.11 shows that the dependence of the mean streamer charge on pressure obeys exponential law with a rather good accuracy:

$$\bar{Q}=\bar{Q}_o \exp(-\beta \cdot \Delta p),\ \beta \sim 10^{-2}/\text{Torr}\ .$$

Thus, considering 20-40 Torr as the typical atmospheric pressure fluctuations, we obtain about 20-40% variations in the charge and, consequently, in energy measurements.

It is possible to compensate these changes by appropriate tuning the high voltage. The dependence of the charge on the high voltage is also exponential:

$$Q=Q_o \exp(\gamma \cdot \Delta U),\ \gamma \sim 2 \cdot 10^{-3}/\text{V}\ .$$

Hence, it should give a feedback coefficient of an order of 5 V/Torr. However, this coefficient depends on the mean charge as the charge characteristic change their slopes with pressure (fig.10). The values of the feedback coefficients obtained from fig.10 are represented in fig.12. For the expected DELPHI operating point ($\bar{Q} \approx 20$pC) it is about 3 V/Torr. So, this demands tuning the high voltage in the range over 100 V.

It is natural to believe the pressure dependence is due to gas density change. Considering the gas to be ideal (PV=NkT), one can estimate the dependence of the streamer charge on temperature:

$$\frac{\delta N}{N} = \frac{\delta P}{P}\Big|_{T=\text{const}} \quad \text{and} \quad \frac{\delta N}{N} = -\frac{\delta T}{T}\Big|_{P=\text{const}},$$

that is the relative temperature dependence is the same as the relative pressure dependence up to a sign. It gives about 3%/°C

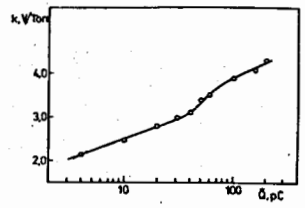

Fig.12. The feedback coefficient to keep the mean charge constant while the pressure changes.

charge dependence and the feedback coefficient of high voltage tuning about -10 V/°C.

From the exponential dependence of the charge on the high voltage, as mentioned above, we obtain the scale of the charge instability due to high voltage fluctuations $\frac{\Delta Q}{Q}=\gamma\cdot\Delta U$, where $\gamma\approx 0.002$ /V.

It is therefore necessary to monitor the pressure, temperature and high voltage ("slow control").

It can be accomplished, for example,[23] by measuring the charge collected by reference tubes containing radioactive sources and operating under the same conditions as the calorimeter tubes.

One way is to tune high voltage for keeping the measured charge of the reference tubes constant (on-line mode).

Another one is simply recording the charge of the reference tubes to correct the calorimeter response (off-line mode). It should be noted that this method demands the calorimeter detectors should be more reliable which is connected with possible remarkable shift of the plateau towards lower voltage for some conditions.

In all these cases the charges collected by the calorimeter modules themselves could be used to provide more direct monitoring and complementary to "slow control".

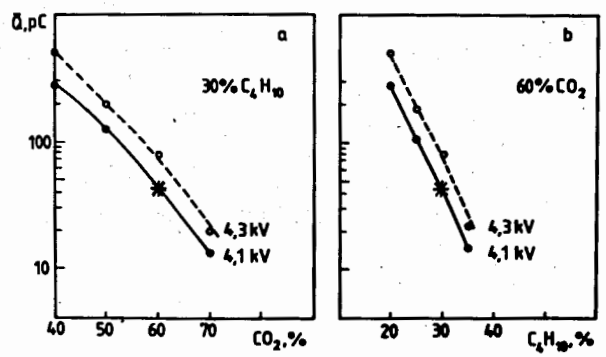

Fig.13. The mean streamer charge change vs the gas mixture variations. The asterisks correspond to the gas mixture Ar:CO_2:i-C_4H_{10}=10:60:30.

7. Accuracy in Preparing the Gas Mixture.

The streamer charge changes with variations in the gas mixture are represented in fig.4,13. The dependence is approximately exponential: $\bar{Q}\approx\bar{Q}_0\exp(-d_1\cdot\Delta C_1-d_2\cdot\Delta C_2)$, where ΔC_1 and ΔC_2 are CO_2 and i-C_4H_{10} percentage deviations. For the gas mixture Ar:CO_2:i-C_4H_{10}=10:60:30 the dependence is considerable (d_1=0.11; d_2=0.19).

Thus the gas system should maintain the percentage with the absolute accuracy not worth than 0.1% and ensure qualitative mixing before the gas is distributed among the calorimeter modules.

8. Streamer Charge Fluctuations.

The streamer charge spectrum is narrower than the proportional one, but it is still rather wide: the dispersion is in the range of ~70-90%. In the DELPHI hadron calorimeter a hadron gives 5-7 streamers per 1 GeV of its energy[18,20]. Thus, the fluctuations of the total collected charge which are due to the specific streamer spectrum shape can be evaluated as:

$$\frac{\delta Q_{TOTAL}}{Q_{TOTAL}}\simeq\frac{\delta Q_{streamer}}{Q_{streamer}}\cdot\frac{1}{\sqrt{N}}\simeq\frac{70\text{-}90\%}{\sqrt{6E(GeV)}}\simeq\frac{30\%}{\sqrt{E(GeV)}},$$

which does not practically change the inner DELPHI calorimeter resolution $\frac{80\%}{\sqrt{E}}$ ($\sqrt{80^2+30^2}\sim 85$).

However, in gas mixtures without good quenching properties the charge dispersion can exceed 100% in the transition region from the limited-proportional to streamer mode. Fig.14 demonstrates the difference in the transition regions for the gases with different quenching properties. For example, in the gas mixture Ar:i-C_4H_{10}=50:50 in the transition region from 3.15 kV to 3.35kV the dispersion is in the range 100-130%. The operation in this region with such a gas would apparently deteriorate the calorimeter resolution to $\frac{90\text{-}95\%}{\sqrt{E}}$. Noteworthy is the abrupt change of the mean charge in this region from 3 to 25 pC.

So, it's preferable to operate calorimeter with a good quenching gas at the beginning of the streamer plateau, where specific streamer fluctuations are minimal.

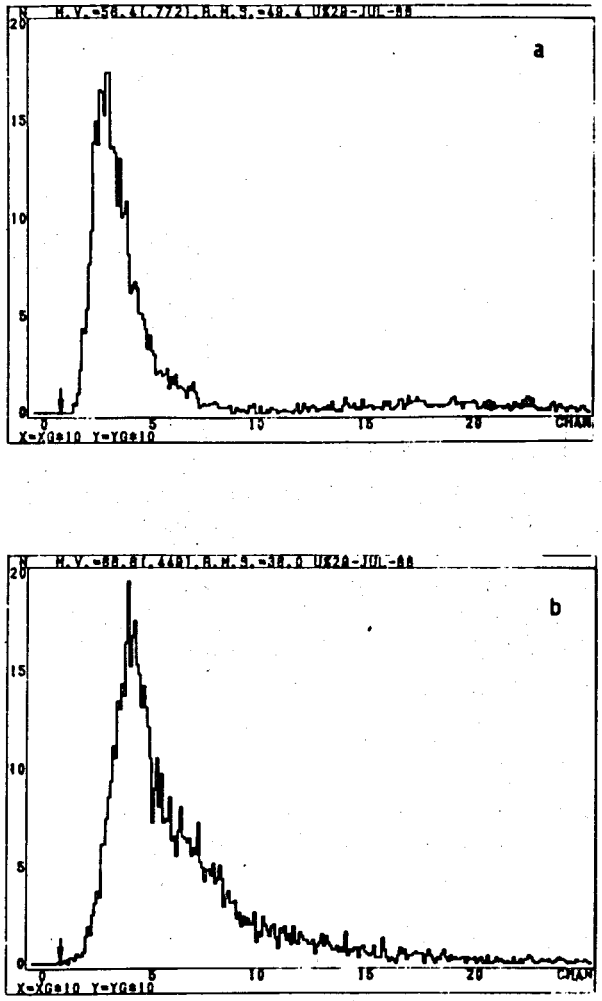

Fig.14. The charge spectra in the transition region from the limited-proportional to streamer mode for the gas mixtures Ar:i-C_4H_{10}=50:50 (a) and Ar:CO_2:i-C_4H_{10}=10:60:30 (b). The signal dispersion is about 120% for the first mixture and about 70% for the second one. The arrow indicates the pedestal (the 16th channel).

9. Geometry Deviations.

This section represents the calculated and experimental data about the influence of different deviations in the detector geometry on the charge value. The contributions of the charge changes to the calorimeter response are presented.

9.1 Pad Position.

It is of importance that the boards with the read-out electrodes should be uniformly pressed to the tube layers, since the charge is read-out from only one side of the tube layer (the other one is simply screened) whereas the division of the induced charge between the read-out electrode and the screen depends on geometric relationships. The electrostatic calculations and the measurements reveal a considerable sensitivity to the gap between the pad and the tube (fig.15): a 1 mm gap results in a 10% decrease in the induced charge .

Assuming that the gaps do not change at a distance of about 20 cm (transverse shower dimension) and taking into account the distribution of the energy deposition along the calorimeter depth[20,21], we obtain the contribution to the energy resolution for the DELPHI calorimeter (5 cm iron layers, averaging over the whole shower length) in the form: $\frac{\sigma_E}{E} \sim 4\% \cdot \sigma_{pad}(mm)$ (σ_{pad}-the dispersion of the pad positions). It was also assumed that the pad deviations between layers are independent. If the displacements are correlated, it's possible to take into account the systematic shift in energy response for different calorimeter towers of ~10% per 1 mm.

It is therefore necessary to guarantee the deviations of the pick-up electrodes to be less than ~1 mm.

All that was discussed concerns the pressing of the screen against the other side of tube layers as well.

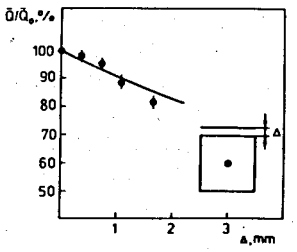

Fig.15. The electrostatic calculations (curve) and the measurements (circles) of the induced charge decrease with the pad removing off the tube surface.

9.2 Detector mechanical tolerances.

The influence of the anode wire displacement from the central position and of the deviations in the cell size on the charge can be calculated from the charge characteristic.

Let the charge be Q_o at the high voltage U_o. This charge is determined by the electrical intensity in the vicinity of the anode wire, and the electrical intensity is determined by the linear charge density on the anode wire $\rho_o = U_o \cdot C_o$, where C_o is the linear capacity. Geometry variations change C_o and thus change the linear charge density: $\Delta\rho = U_o \cdot \Delta C$.

And from the charge characteristic ($Q = Q_o \cdot e^{\gamma \cdot \Delta U}$) it is easy to extract the charge dependence on the linear charge density at the anode wire:

$$\frac{\Delta Q}{Q_o} \simeq \gamma \cdot \Delta U = \gamma \cdot \frac{\Delta \rho}{C_o}$$

Hence we obtain the dependence of the charge on the linear capacity in the form:

$$\frac{\Delta Q}{Q_o} \simeq \gamma \cdot U_o \frac{\Delta C}{C_o} \quad .$$

The calculations of the linear capacity changes in the case of the anode wire displacement and the cell size variations are represented in fig.16.

The values for $\gamma \cdot U_o$ (the gas mixture $Ar:CO_2:i\text{-}C_4H_{10} = 10:60:30$) in the limited-proportional ($U_o = 3.8$kV) and streamer ($U_o = 4.3$kV) modes can be extracted from fig.4: they are 14 and 9.1 respectively.

Fig.17 presents the results of the final calculations and the measurements for the case of the anode wire displacement (the charge read-out from the anode wire).

It should be noted that besides the variation of the avalanche and the streamer charge the anode wire displacement can cause the change in the charge division between the read-out electrode and the screen. The calculated change in the induced charge fraction with the displacement of the anode wire to the screen is presented in fig.18. It is seen that the changes in the induced charge division are more essential than the streamer (avalanche) charge variation itself.

Fig.16. The change in the detector linear capacity at different geometry deviations: a) anode wire displacement; b,c) cell size deviations.

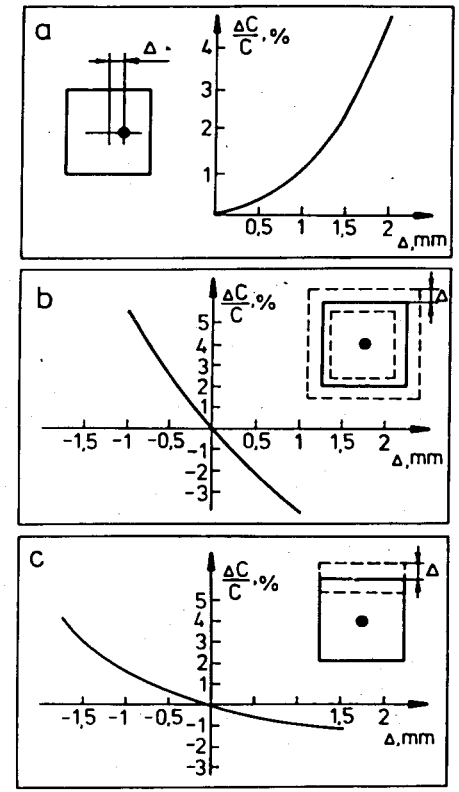

Thus, the anode wire displacement of 1 mm results in the 20% charge change and the cell size variation of 1 mm results in the charge change ≤40%. All these changes are substantially less than the streamer charge fluctuations. (The statistical contribution of geometrical deviations to the calorimeter resolution can be estimated as well as in the case of specific charge fluctuations.)

However, if these geometrical deviations have the systematic behavior, the tolerance requirements become more rigid. The systematic deviations can in principle result from technology of assembling, when detectors with similar features are grouped in different modules of the calorimeter. To keep the charge variations in different modules under the intrinsic 8% level, it

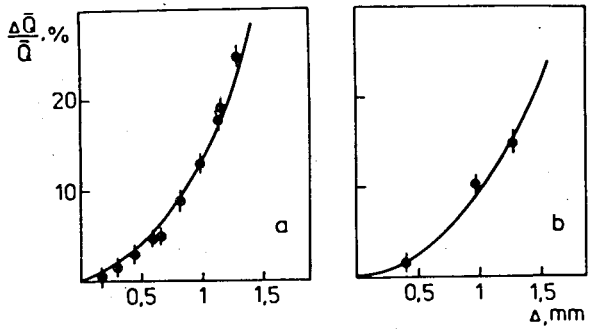

Fig.17. The calculations (curves) and the measurements (circles) of the anode charge change vs the anode wire displacement. The gas mixture Ar:CO_2:i-C_4H_{10}=10:60:30.
a) U=3.8kV (the limited-proportional mode)
b) U=4.3kV (the streamer mode)

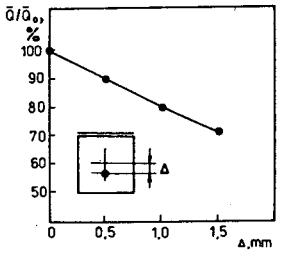

Fig.18. The calculated change in the charge fraction induced on the pad for the anode wire displacement.

is necessary that the mean deviations in the detector geometry for different modules ($\bar{\Delta}=\frac{1}{L}\int_0^L \Delta(l)dl$, where L~1 km is the range of the total detector length in one module) do not differ by more than ~200 μm for the anode wire displacement and by ~100 μm for the cell size variations.

It should be kept in mind that the local geometric deviations do not change the calorimeter resolution but they are very critical for the stable detector operation. For example, fig.19 shows that the self-sustaining discharge occurs at lower voltage as the anode wire displacements increase.

The 20% charge change is equivalent to the ~ 100 V high voltage shift, which is already comparable with ~500 V plateau for these tubes. Thus, we estimate the local tolerance for the detector design as the following: the

Fig. 19. The detector current for different anode wire displacements. The detector was exposed to the ^{90}Sr β-source of intensity ~200 $cm^{-2}s^{-1}$. The numbers give the displacements in mm. The gas mixture Ar:i-C_4H_{10} = 25:75 was used; the knee of the singles rate curve was at 4.4 kV.

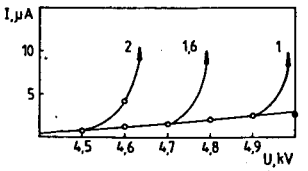

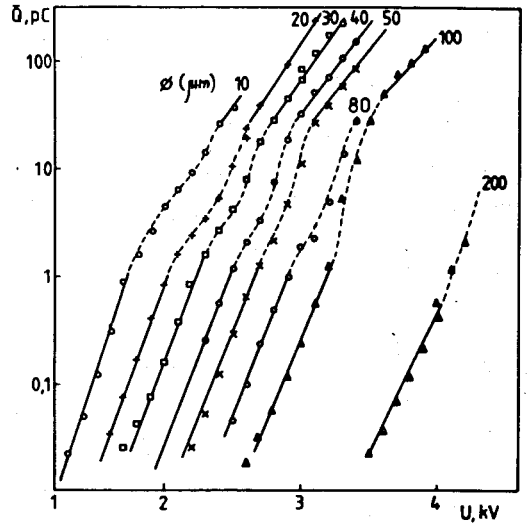

Fig.20. The charge characteristics for different wire diameters (the figures represent the anode wire diameters; the dashed lines indicate the transition region from the proportional mode to the streamer one). The gas mixture Ar:i-C_4H_{10}:=50:50 was used.

anode wire displacement should be less than 1mm, the cell size variations should be less than 500 μm.

Then to estimate the influence of the anode wire diameter deviations on the collected charge, the measurements were done with wires of different diameters. Fig.20 shows that the diameter change results in a simple shift of the charge characteristic curves. The dependence of the shift on the anode wire diameter (fig.21) allows us to estimate the dependence of the charge on the anode wire diameter.

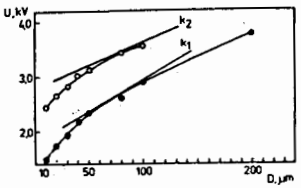

Fig.21. The high voltage vs the anode wire diameter on condition that the mean charge is kept constant (Q = 0.1 pC(•); Q = 30 pC(○)). The coefficients are k_1 = 12 V/μm and k_2 = 8 V/μm.

A small diameter deviation ΔD results in the high voltage shift $\Delta U = k \cdot \Delta D$ and the charge change is therefore:

$$\frac{\Delta Q}{Q_o} \simeq \gamma \cdot \Delta U \simeq \gamma \cdot k \cdot \Delta D = \gamma \cdot k \cdot D_o \cdot \frac{\Delta D}{D_o}$$

The charge change for detector with the 80 μm anode wire diameter is $\frac{\Delta Q}{Q_o} \simeq 2 \cdot \frac{\Delta D}{D_o}$ in the streamer mode and $\frac{\Delta Q}{Q_o} \simeq 5 \cdot \frac{\Delta D}{D_o}$ in the proportional mode.

Thus, the tolerable local diameter deviations in streamer mode should be less than 10%, i.e. about 8 μm for the 80 μm diameter, and the tolerable systematic diameter changes should be less than 2%, i.e. about 2μm for the 80 μm diameter.

10. Conclusion.

Different factors which influence the operation of the plastic streamer tubes for the DELPHI hadron calorimeter were considered.

The charge scaling was observed for tested gas mixtures, which means that stability of operation depends generally on average streamer charge, but not on a gas mixture composition. However, mixtures with good quenching should be given preference as they provide weak sensitivity to mechanical irregularities of the detector. Streamer mode as well ensures more weak signal dependence on detector geometry with regard to proportional one.

The contributions to the response of the calorimeter were estimated. The main numerical results are collected in Table 1 (note that the statistical contributions should be added quadratically to the intrinsic calorimeter resolution $\sim \frac{80\%-100\%}{\sqrt{E(GeV)}}$).

Table 1.

cause of the influence	scale of the charge change $\frac{\Delta Q}{Q}$ (readout from pick-up electrodes)	estimated contributions to the energy measurement bias (system.) and resolution (statistical)		tolerable * deviations of parameter (or compensation method)
pressure fluctuations	-1% per 1 Torr ($-8 \cdot \frac{\Delta P}{P}$)	-1% per 1 Torr	syst	high voltage tuning +3 V/Torr
temperature fluctuations	+3% per 1 °C ($+8 \cdot \frac{\Delta T}{T}$)	+3% per 1 °C	syst	ΔT<1 °C; high voltage tuning -10 V/°C
accuracy of preparing the gas mixture	20% per ΔC=1% ($\sim 6 \cdot \frac{\Delta C}{C}$)	20% per ΔC=1%	syst	ΔC<0.1%
high voltage instability	+0,2% per 1 V ($\sim 8 \cdot \frac{\Delta U}{U}$)	+0.2% per 1 V	syst	ΔU<10 V
aging	-0.06% per year at ~1 $cm^{-2}s^{-1}$ radiation load	-0.06% per year	syst	———
magnetic field	-3% per 1 T	-3% + (20-30)% per 1T**	syst	calibration with magnetic field
self-sustining discharge	<2% at I~10 μA	<0.5%	syst	I<10 μA
streamer charge fluctuations	~80% (up to ~130% in the transition region in the gases with weak quenching)	$\frac{30\%}{\sqrt{E}}$ (up to $\frac{50\%}{\sqrt{E}}$)	stat	use of the gases with weak quenching is not desired
pad (screen) displacement	10% per 1 mm ($\sim 0.5 \frac{\Delta X}{X}$)	4-10% per 1 mm	syst	ΔX<1 mm
anode wire displacement	20% per 1 mm ($\sim 1 \frac{\Delta X}{X}$)	$\frac{8\%}{\sqrt{E}}$ per 1 mm	stat	Δx<1,5mm (from the operation stability)
		20% per 1 mm	syst	$\overline{\Delta x}$<200 μm

cause of the influence	scale of the charge change $\frac{\Delta Q}{Q}$ (readout from pick-up electrodes)	estimated contributions to the energy measurement bias (system.) and resolution (statistical)		tolerable deviations * of parameter (or compensation method)
cell size variations	≤40% per 1 mm ($\sim 2\frac{\Delta X}{X}$)	$\frac{15\%}{\sqrt{E}}$ per 1 mm	stat	ΔX<.5 mm (from the operation stability)
		40% per 1 mm	syst	$\overline{\Delta X}$<100 μm
deviations of the anode wire diameter	streamer: ~2.5% per 1 μm ($\sim 2\frac{\Delta D}{D}$)	$\frac{1\%}{\sqrt{E}}$ per 1 μm	stat	ΔD<10 μm (from the operation stability)
		2.5% per 1 μm	syst	$\overline{\Delta D}$<2 μm

(*) - obtained at following conditions: for syst. - the influence should be much less than 8-10% - the intrinsic calorimeter resolution at 100 GeV; the local deviations in the geometry are restricted by the tubes operation stability demands: 20% charge change is equivalent to ~100 V high voltage shift which is already comparable with ~500 V plateau; averaging ($\bar{\Delta}$) is made over the detector length ~1km, corresponding to a single module of the calorimeter.

(**) - the estimated calorimeter response change due to the magnetic field influence on the shower development.

It is seen from Table 1 that:

- the atmospheric pressure and detector temperature fluctuations result in large response changes, and they should be monitored;
- to exclude remarkable systematic bias of the calorimeter response for different modules, the detector production procedure should provide the invariable detector geometry for long periods of the time.

Acknowledgements.

The authors are grateful to G.V.Micelmacher for the support of this work, to V.D.Ryabtsov, V.G.Shelkov, V.L.Malyshev, E.Sevenyan for the assistance in the measurements and to the whole DELPHI hadron calorimeter group and D.M.Khazins for the fruitful discussions of the questions concerned.

References.

1. DELPHI, Technical Proposal, CERN/LEPC/83-66
2. E.Iarocci, NIM 217(1983)30
3. G.D.Alekseev et al., NIM A269(1988)652
4. SLD Design Report, SLAC-Report-273, 1984
5. M.Mishina, in Proc. of the 2nd Gas Calorimeter Workshop, Fermilab, 1985 (ed. M.Atac)
6. A.S.Vodopyanov et al., JINR, D1-87-328, Dubna, 1987
7. G.Battistoni et al., Phys.Lett. 118B(1982)461
8. Yu.P.Guz et al., IHEP 86-208, Serpukhov, 1986.
9. G.Bagliesi et al., CERN-EP/87-124, 1987
10. H.Bergstein et al.,PITHA 87/16, 1987
11. G.A.Akopdjanov, IHEP 88-145, Serpukhov, 1988
12. G.D.Alekseev et al., NIM 177(1980), 385
13. H.Raether. Electron Avalanches and Breakdown in Gases. (Butterworths, London, 1964)
14. G.Battistoni et al., NIM 164(1979)57
15. N.A.Filatova et al., NIM A243(1986)91
16. G.D.Alekseev et al., JINR E13-87-399, Dubna, 1987
17. J.Va'vra, NIM A252(1986)547
18. G.D.Alekseev, L.G.Tkachev, JINR E13-84-640, Dubna, 1984
19. G.D.Alekseev, A.V.Korytov, NIM A268(1988)151
20. G.A.Akopdzhanov et al., IHEP 86-62, Serpukhov, 1986
21. M.Holder et al., NIM 151(1978)69
22. G.D.Alekseev et al.,JINR E1-89-236, Dubna, 1989
23. K.De Winter et al. CERN-EP/89-32, 1989.

Received by Publishing Department
on April 13, 1989.